Biogeochemistry (2006) 80:217–231
DOI 10.1007/s10533-006-9019-5

ORIGINAL PAPER

The global-scale temperature and moisture dependencies of soil organic carbon decomposition: an analysis using a mechanistic decomposition model

Takeshi Ise · Paul R. Moorcroft

Received: 1 September 2005 / Accepted: 21 February 2006 / Published online: 5 June 2006

Abstract Since the decomposition rate of soil organic carbon (SOC) varies as a function of environmental conditions, global climate change is expected to alter SOC decomposition dynamics, and the resulting changes in the amount of CO_2 emitted from soils will feedback onto the rate at which climate change occurs. While this soil feedback is expected to be significant because the amount of SOC is substantially more than the amount of carbon in the atmosphere, the environmental dependencies of decomposition at global scales that determine the magnitude of the soil feedback have remained poorly characterized. In this study, we address this issue by fitting a mechanistic decomposition model to a global dataset of SOC, optimizing the model's temperature and moisture dependencies to best match the observed global distribution of SOC. The results of the analysis indicate that the temperature sensitivity of decomposition at global scales (Q_{10}=1.37) is significantly less than is assumed by many terrestrial ecosystem models that directly apply temperature sensitivity from small-scale studies, and that the maximal rate of decomposition occurs at higher moisture values than is assumed by many models. These findings imply that the magnitude of the soil decomposition feedback onto rate of global climate change will be less sensitive to increases in temperature, and modeling of temperature and moisture dependencies of SOC decomposition in global-scale models should consider effects of scale.

Keywords Carbon cycling · Climate change · Modeling · Decomposition · Q_{10} · Likelihood

T. Ise (✉) · P. R. Moorcroft
Department of Organismic and Evolutionary Biology, Harvard University, 22 Divinity Avenue, Cambridge, MA 02138, USA
e-mail: ise@fas.harvard.edu

Introduction

Increased radiative forcing arising from rising atmospheric CO_2 concentrations is expected to increase soil temperatures, accelerating rates of soil organic carbon (SOC) decomposition, which, in turn, will increase the rate at which CO_2 accumulates in the atmosphere (Schimel et al. 1994; Kirschbaum 1995; Jobbagy and Jackson 2000). Since the amount of carbon stored in soil is estimated to be 1500 PgC, approximately double as much as that in the atmosphere (Schlesinger 1997), the potential magnitude of this feedback is strong. Due to this positive feedback, understanding the change in SOC decomposition rate under climate change is considered one of the critical aspects of climate modeling (IPCC 2001). However, temperature and moisture dependencies of SOC decomposition is highly variable (Holland et al. 2000; Chimner and Welker 2005) and hotly debated (Giardina and Ryan 2000; Knorr et al. 2005).

The potential importance of SOC decomposition feedbacks onto climate has been highlighted in recent coupled biosphere–atmosphere model simulations. Climate models that exclude SOC feedbacks predict that a doubling of CO_2 concentrations will result in temperature increases of 2.8–4.2°C in 2100 (Manabe and Wetherald 1987; Hansen et al. 1988; Schlesinger and Zhao 1988), while a study using a coupled biosphere–atmosphere model predicts that a doubling of CO_2 concentrations will result in a 5.5°C increase in average global temperature primarily due to a loss of terrestrial carbon storage (Cox et al. 2000; Cox 2001). However, recent analysis with a multiple SOC pool model suggests that the positive feedback of SOC is less intense (Jones et al. 2005). Understanding the environmental dependencies of SOC decomposition is therefore essential for improving predictions of future climate change. This is particularly true for northern peatland ecosystems that contain an estimated 455 PgC SOC (Gorham 1991), approximately one-third of total global SOC storage. These ecosystems have been experiencing significant warming over the past few decades: winter and spring temperatures in west-central and northwestern Canada, and most of Siberia have increased by 2–3°C over the latter half of the 20th century (Environment Canada 1995), and these regions are expected to experience further warming as anthropogenic climate forcing continues. Recent projections by four general circulation models (GCMs) predict winter and summer temperature rises of 6–10°C and 4–6°C, respectively, under a doubled-CO_2 climate (Stocks et al. 1998). Moreover, SOC decomposition rates may change particularly rapidly in areas with high SOC content, such as northern peatlands (Bellamy et al. 2005; Schulze and Freibauer 2005).

Despite the importance of SOC dynamics for predicting future climate change, the response of SOC decomposition to changes in temperature and moisture at global scales remains poorly characterized. Observations of the relationship between temperature and SOC decomposition rates come from either restricted regions or relatively short-term laboratory incubations (e.g., Winkler et al. 1996; Niklinska et al. 1999) that are highly variable (Holland et al. 2000). As a result, there is significant variation in decomposition parameters used in terrestrial ecosystem models. For example, in the Century decomposition formulation (Parton et al. 1987, 1988, 1993; Schimel et al. 1994, 1996) that is the basis for a number of soil decomposition models, including those in the CASA (Potter et al. 1993), MC1 (Bachelet et al. 2001), and ED (Moorcroft et al. 2001) models, the Q_{10} for SOC decomposition in the biologically relevant range of 0–30°C, is 2.49 (Fig. 1a), while the decomposition of the Triffid ecosystem model used by HadCM3LC general circulation model (Cox et al. 2000; Cox 2001; Jones et al. 2003) has a Q_{10} of 2.0. Under these assumptions, future temperature rise markedly intensifies microbial activity and resulting decomposition rates, and the positive feedback onto the temperature rise is strong. For example, using the Century formulation in CASA, Potter and Klooster (1997) found that a globally uniform increase in surface air temperature of 1°C would cause net loss of 5% of SOC pool, and Cox et al. (2000) predicted the warming from 2,000 to 2,100 will result on 14% loss of SOC. Because these simulations use relationships of temperature and SOC decomposition derived from small-scale studies, this temperature dependency may not hold at larger spatial and longer temporal scales (Giardina and Ryan 2000; Valentini et al. 2000)

The effects of moisture availability also vary significantly: in the original Century formulation (Parton et al. 1987), soil decomposition is fastest when precipitation equals potential evapotranspiration (Fig. 1b), while in Triffid (Cox 2001) soil moisture is assumed optimum when the degree of saturation is mid-way between the permanent wilting point and complete saturation. Interpretation of moisture dependence at global scales can be very different from local experimental studies because geomorphological heterogeneity that strongly affects water availability is implicitly included in the large grid cells of global-scale models.

In this study, we estimate the global-scale temperature and moisture dependencies of SOC decomposition by fitting the predictions of a simple, mechanistic decomposition model, implemented within a series of grid cells covering the terrestrial land surface, to the observed global-scale spatial distribution of SOC. The decomposition model is forced by litter inputs calculated from a simple empirical model of net primary productivity, with the partitioning among the quickly decomposing

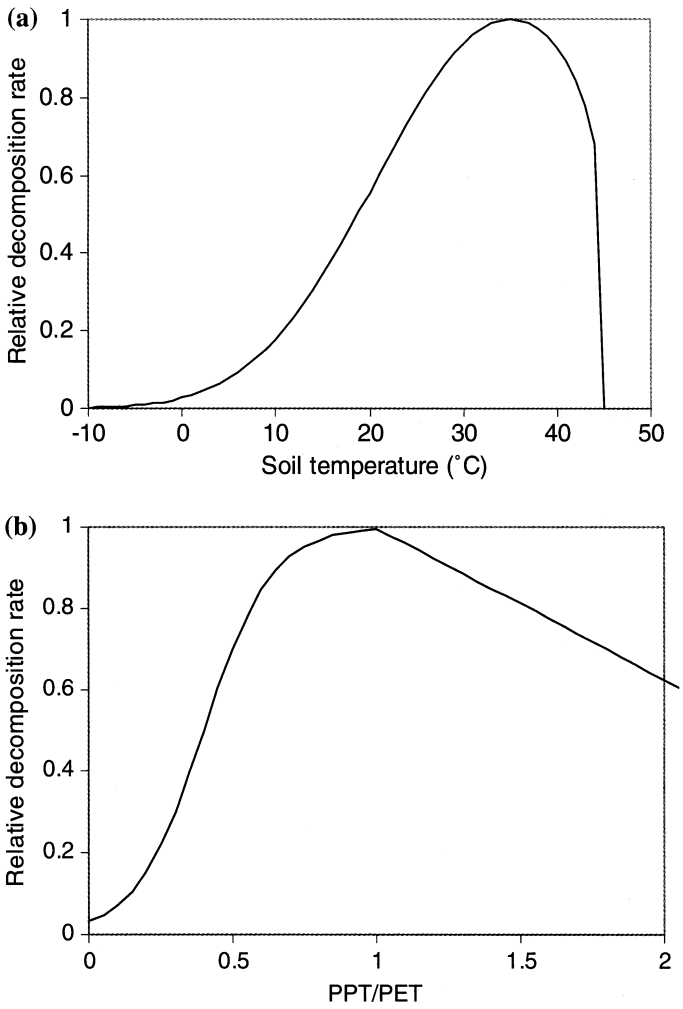

Fig. 1 Assumed temperature and moisture dependencies of SOC decomposition in Century model (Parton et al. 1987). (**a**) Temperature dependency. (**b**) Moisture dependency. The relative decomposition rate is a function of the ratio between precipitation (PPT) and potential evapotranspiration (PET)

metabolic SOC pool, slowly decomposing structural SOC pool, and recalcitrant slow/passive SOC pool varying as a function of vegetation type and land-use class within each grid cell. The temperature and moisture dependencies of decomposition are then estimated by temperature and moisture parameters of the decomposition model to optimize the match between the model's predictions of SOC density for each grid cell and a global dataset of SOC measurements. With this inverse analysis, calibrated decomposition parameters are presented, and implications for global-scale modeling are made.

Model

The decomposition model is a simple Century-based mechanistic decomposition model used by Moorcroft et al. (2001), based on analyses of Parton et al. (1987, 1988, 1993), Potter et al. (1993), Schimel et al. (1994, 1996) and Bolker et al. (1998), and consists of: (1) a metabolic pool of quickly decomposing labile plant materials such as foliage and fine roots, (2) a structural pool of woody plant parts and other slowly decomposing plant materials, and (3) a slow/passive pool of chemically recalcitrant materials derived from transformed structural soil pool (Fig. 2). SOC in each compartment decays exponentially, with the turnover rates of the three pools under optimal environmental conditions being 11.0, 4.5, and 0.104 y^{-1}, respectively. These intrinsic decomposition rates of the pools are modified by the soil temperature and moisture conditions within each grid cell. As in many terrestrial ecosystem models (e.g.,Cox 2001; Moorcroft et al. 2001; Jones et al. 2005), the effects of soil texture on SOC decomposition are not represented.

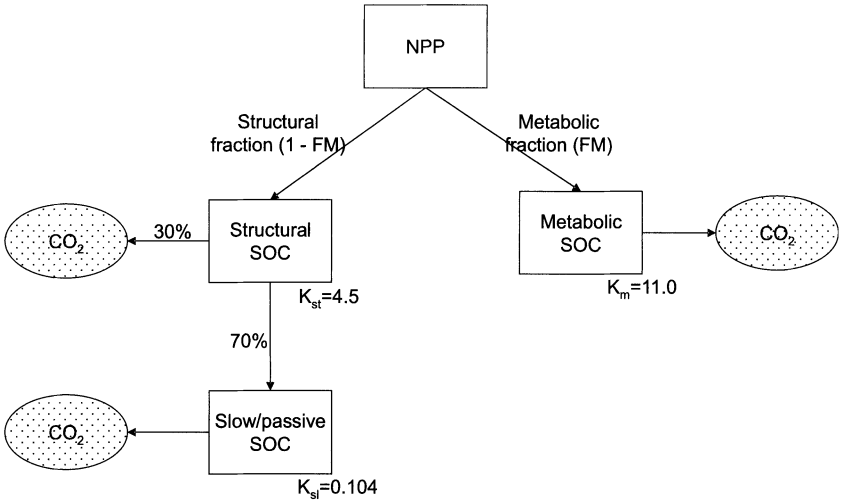

Fig. 2 Schematic representation of decomposition model, modified from Parton et al. (1987), according to Bolker et al. (1998). NPP is assumed to be equal to the litter input for a long-term, steady state condition. Litter input to soil is divided to metabolic and structural SOC fractions according to CASA (Potter et al. 1993) parameters for each biome. Seventy percent of Structural SOC pool is gradually transformed into Slow/passive SOC pool. Each pool has a unique rate of decomposition

Partitioning of litter to each pool is determined by chemical properties of the material, specifically the lignin-to-nitrogen ratio (LN) and carbon-to-nitrogen ratio (CN). Mathematically, the model's dynamics are expressed by the following equations:

$$C_{\text{total}} = C_{\text{met}} + C_{\text{str}} + C_{\text{slow}} \tag{1}$$

C_{total} is the total SOC in the grid cell and C_{met}, C_{str}, and C_{slow} are SOC densities in metabolic, structural, and slow/passive pools, respectively. The rates of change of SOC in each pool are given by:

$$\frac{dC_{\text{met}}}{dt} = \text{NPP}F_{\text{met}} - Ak_{\text{met}}C_{\text{met}} \tag{2}$$

$$\frac{dC_{\text{str}}}{dt} = \text{NPP}(1 - F_{\text{met}}) - Ak_{\text{str}}C_{\text{str}} \tag{3}$$

$$\frac{dC_{\text{slow}}}{dt} = 0.7Ak_{\text{str}}C_{\text{str}} - Ak_{\text{slow}}C_{\text{slow}} \tag{4}$$

NPP is total net primary productivity of the grid cell. F_{met} is a fraction by which NPP goes into metabolic pool. NPP and F_{met} are described in detail below. The function A modifies the intrinsic decomposition rate for each SOC pool based on the temperature and moisture conditions within the grid cell. Consistent with the analysis of Bolker et al. (1998), there is no transfer of material between the metabolic and slow/passive SOC pools. The amount of SOC in each pool is assumed to reach an equilibrium with constant input and output rates, and we solve the differential equations (2–4) for an equilibrium.

Effects of temperature and moisture

In the Century model the effects of temperature and moisture are multiplicative, i.e.,

$$A = \text{Td}\,\text{Md} \tag{5}$$

where Td and Md are functions describing the effects of temperature and moisture on decomposition rate. As in the original Century formulation (Parton et al. 1987), all pools exhibit the same environmental dependencies and effects of temperature and moisture are independent. The effect of temperature, Td, is a dimensionless number between 0 and 1 and calculated according to the following functional form of Parton et al. (1987):

$$\text{Td} = t_2 t_1^{\wedge}\, \text{td}_a \tag{6}$$

where

$$t_1 = \frac{T_{\max} - T_{\text{m}}}{T_{\max} - T_{\text{opt}}} \tag{7}$$

and

$$t_2 = \exp\left[\frac{td_a}{td_b}(1 - t_1^{\wedge}\, td_a)\right] \quad (8)$$

T_m is mean monthly temperature from the dataset, T_{max} is the temperature at which decomposition stops because it is too high for biological activity, T_{opt} is the optimal temperature for decomposition (i.e., Td=1 when T_m=T_{opt}). For this study, T_{max} and T_{opt} are set to 45 and 35°C, respectively, identical to the original Century formulation. The parameters td_a and td_b are the model parameters optimized later in this study. The Td function with original Century td_a and td_b values (td_a=0.2 and td_b=2.63) is plotted in Fig. 1a.

Md is also calculated according to Parton et al. (1987):

$$Md^* = \frac{1}{1 + md_a \exp\left[-md_b \frac{PPT}{PET}\right]} \quad (PPT \le PET) \quad (9)$$

$$Md^* = \frac{1}{1 + md_a \exp\left[-md_b \frac{PPT}{PET}\right]} - 0.375\left[\frac{PPT}{PET} - 1\right] \quad (PPT>PPT) \quad (10)$$

$$Md = \frac{Md^*\left(\frac{PPT}{PET} | md_a, md_b\right)}{Md^*\left(\frac{PPT}{PET} = 1 | md_a, md_b\right)} \quad (11)$$

where PPT is monthly precipitation (mm) from the dataset, and PET is possible evapotranspiration (mm) calculated according to Malmstrom (1969). When PPT=PET, moisture conditions are considered optimal and Md is 1. If PPT<PET, the environment is dry and decomposition is moisture limited, and when PPT>PET, the decomposition rate declines linearly with increasing precipitation, reaching a minimum when PPT/PET ratio is 3.67 for the original Century values of md_a and md_b (Fig. 1b). Whereas Td=1 when T_m=T_{opt} regardless of the values of td_a and td_b, Md^* will not be 1 at the optimal wetness when md_a and md_b are changed from their original values. To make Md=1 when moisture condition is optimum, the Md^* curve is rescaled by dividing Md^* by the highest value of Md^* calculated using the original Century equation (Eq. 11). Consistent with Clymo's (1984) estimate that decomposition rates under an anaerobic condition are three orders of magnitude smaller than that under an aerobic condition, we assume that the minimum values of Td and Md are 0.001.

Litter inputs

The carbon decomposition model is forced with litter inputs calculated from a simple terrestrial productivity model. NPP within each climatological grid cell is estimated by using a modified version of Miami model (Friedlingstein et al. 1992; Yang et al. 2002), which predicts total NPP globally from precipitation and mean annual ''biotemperature'' (only monthly temperatures in 0–30°C range are accounted for mean annual biotemperature), instead of simple mean temperature used by the original Miami model (Lieth 1975). Estimates by this simple NPP model are reasonable for major biomes (Dai and Fung 1993), and we assume that this model is satisfactory to reproduce fundamental environmental dependencies of NPP. The NPP for each grid cell is calculated using the 1961–1990 0.5° resolution global monthly temperature and precipitation of New et al. (2000), and the estimation of global total NPP is 63.2 PgC/year, which is within the range of NPP estimates produced by 17 global models (44.4–66.3 PgC/year) described in an intercomparison study (Cramer et al. 1999). Since our SOC decomposition model is not vertically stratified, we do not distinguish above- and below-ground NPP.

Litter inputs are then calculated by partitioning the NPP between woody and non-woody material, the partitioning depending on the Carbon to Nitrogen ratios (CN) and Lignin Fraction (LF) of the ecosystem, which varies as a function of the vegetation type and land-use fraction within each grid cell (Table 1). The density of organic nitrogen produced in a year is NPP divided by CN, and that of lignin is NPP multiplied by LF. The metabolic fraction of NPP is determined by 0.85–0.018·(lignin density)/(nitrogen density) (Parton et al. 1987). The calculated metabolic fractions for different ecosystem types are given in Table 1. The vegetation type within each 0.5×0.5° grid cell is specified using the IBIS vegetation cover (Foley et al. 1996), and the fraction of agricultural land for each grid cell is specified from the 0.5×0.5° global dataset of Ramankutty and Foley (1998). The CN and LF of litter for each vegetation type (including cropland) are then specified using the

Table 1 Vegetation classification used in IBIS (Foley et al. 1996) and chemical characteristics of each biome derived from CASA (Potter et al. 1993)

Vegetation class	C:N ratio (CN)	Lignin fraction (LF)	Metabolic fraction
1. Tropical evergreen forest	40	0.2	0.71
2. Tropical deciduous forest	50	0.2	0.67
3. Temperate broadleaf evergreen forest	40	0.2	0.71
4. Temperate needleleaf evergreen forest	80	0.25	0.49
5. Temperate deciduous forest	50	0.2	0.67
6. Boreal evergreen forest	80	0.25[a]	0.49
7. Boreal deciduous forest	50	0.2[a]	0.67
8. Evergreen/deciduous mixed forest	65	0.22	0.59
9. Savanna	50	0.15	0.72
10. Grassland/steppe	50	0.1	0.76
11. Dense shrubland	65	0.2	0.62
12. Open shrubland	65	0.2	0.62
13. Tundra	50	0.15	0.72
14. Desert	65	0.2	0.62
15. Cropland	40	0.1	0.78
16. Polar/rock/ice[b]	100	1.0	–

[a] Modified later in trial TdMdfit-chem

[b] Unused

estimates of Potter et al. (1993). The CN and LF values for each grid cell are calculated as a weighted sum of potential vegetation value and crop value within the grid cell, i.e.:

$$\mathrm{CN} = \mathrm{CN}_{\mathrm{pot}}(1 - F_{\mathrm{crop}}) + \mathrm{CN}_{\mathrm{crop}}F_{\mathrm{crop}} \quad (12)$$

$$\mathrm{LF} = \mathrm{LF}_{\mathrm{pot}}(1 - F_{\mathrm{crop}}) + \mathrm{LF}_{\mathrm{crop}}F_{\mathrm{crop}} \quad (13)$$

where $\mathrm{CN}_{\mathrm{pot}}$ is the CN for potential vegetation, $\mathrm{CN}_{\mathrm{crop}}$ is the CN for cropland, F_{crop} is the fraction of cropland in a grid cell, $\mathrm{LF}_{\mathrm{pot}}$ is the LF for potential vegetation, and $\mathrm{LF}_{\mathrm{crop}}$ is the LF for cropland.

Analysis

We begin by evaluating the ability of the mechanistic decomposition model run with original Century parameter values for the temperature and moisture functions (Orig) to reproduce the global distribution of SOC, comparing the model's predictions of the equilibrium amounts of SOC in each grid cell calculated using Eqs. 2–4, to the 0.5° observed soil carbon density dataset (Global Soil Data Task 2000) shown in Fig. 3a. We use SOC density (kg m^{-2}) for top 1 m of soil as the observed value of SOC. Note that while the Century formulation is designed to simulate SOC in the top 20 cm of soil, here we assume that, consistent with the analyses of Fang et al. (2005) and Burke et al. (2003), the same Td and Md relationship holds to 1 m in depth. A series of four optimizations is then performed: in the first (Tdfit), the temperature parameters ($\mathrm{td_a}$ and $\mathrm{td_b}$) are optimized while the moisture parameters are kept at their original Century values; in the second (Mdfit), the moisture parameters ($\mathrm{md_a}$ and $\mathrm{md_b}$) are optimized while the temperature parameters are kept at their original Century values; in the third (TdMdfit), both the temperature and moisture parameters are optimized simultaneously; in the last (TdMdfit-chem), the optimization is identical to TdMdfit except that TdMdfit-chem uses modified litter quality for boreal forests.

The models are fitted to the SOC observations using maximum likelihood (Edwards 1992). Analysis of the residuals indicates that the distribution of observations around the model predictions is highly non-normal, so the likelihood is calculated assuming a gamma distribution of error that captures the distribution of observation outliers around the model predictions (e.g., see Fig. 5d). Thus, the likelihood for each grid cell is calculated as:

$$L(x, y) = \frac{D^{a-1}}{b^a \Gamma(a)} \exp\left[-\frac{D}{b}\right] \quad (14)$$

where (x, y) is the latitude and longitude of the grid cell, a and b are parameters for gamma error distribution, and D is the deviation of predicted total SOC from observed SOC density for the grid cell ($|C_{\mathrm{total}}^{\mathrm{predicted}} - C_{\mathrm{total}}^{\mathrm{observed}}|$). This yields the following log-likelihood function:

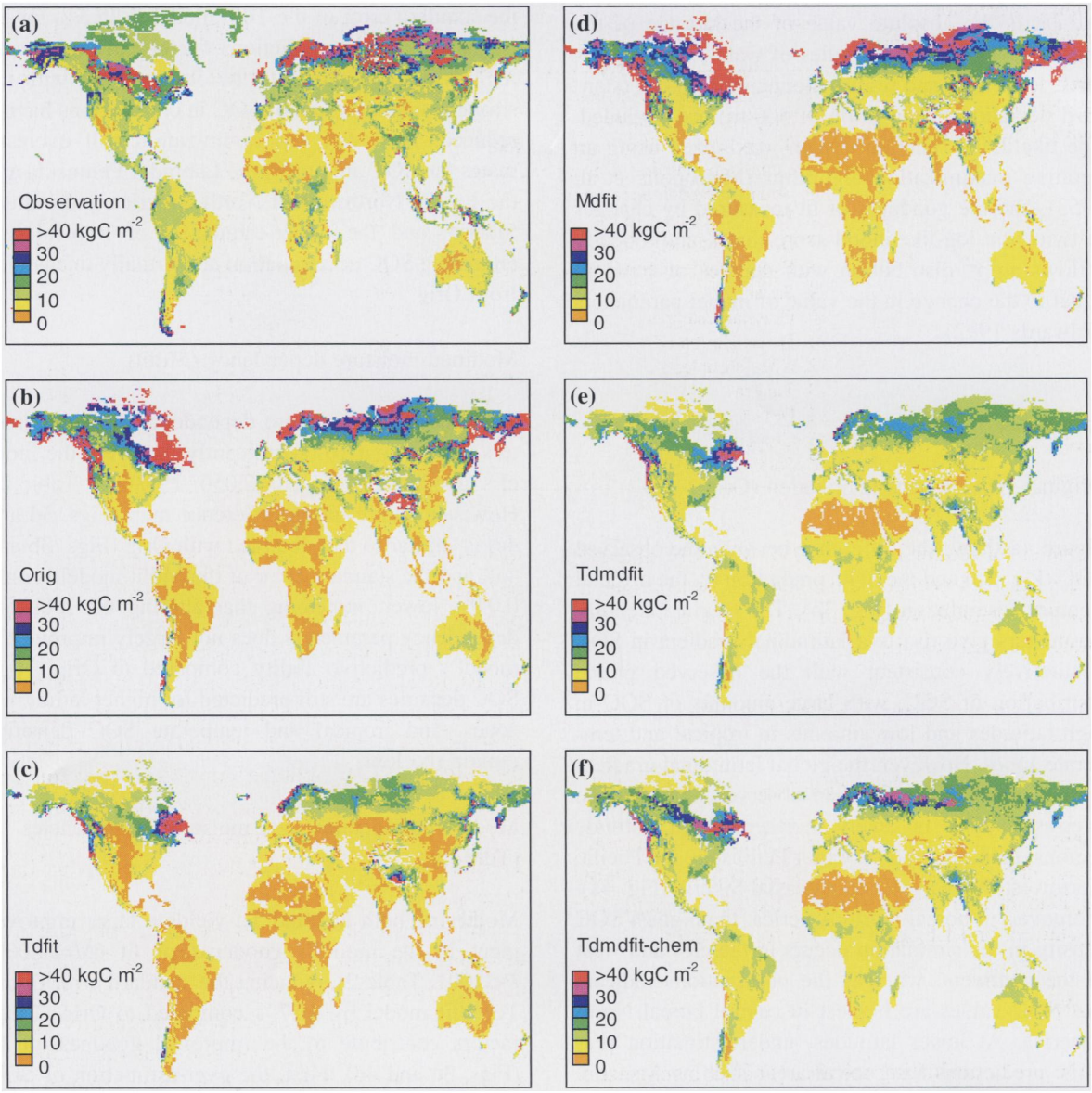

Fig. 3 (**a**) Observed global SOC density [kgC m^{-2}] from Global Soil Data Task (2000). (**b**) Orig: simulated global SOC density with original Century parameters. (**c**) Tdfit: simulated global SOC density with fitted temperature dependency. (**d**) Mdfit: simulated global SOC density with fitted moisture dependency. (**e**) Tdmdfit: simulated global SOC density with fitted temperature and moisture dependencies. (**f**) Tdmdfit-chem: simulated global SOC density with fitted temperature and moisture dependencies with altered litter chemistry in lowland boreal region

$$l(x, y) = -a \ln b - \ln[\Gamma(a)] + (a-1)\ln D - \frac{D}{b} \tag{15}$$

Since the area of the grid cells varies, the likelihood value for each grid cell is scaled by a homolographic (true-area) projection scheme, and summed to give the total likelihood for the all terrestrial grid cells:

$$l = \sum_{x=1}^{360} \sum_{y=1}^{720} l(x, y) h(x) \tag{16}$$

where

$$h(x) = \cos\left[89.75 - \frac{\text{lat}}{2}\right] \tag{17}$$

and lat is the absolute value of the latitude of the center of the grid cell. Bodies of water, extreme deserts, ice sheets and highly mountainous areas (standard deviation of elevation >1,500 m) are excluded. The likelihood function is then maximized using an iterative maximization algorithm (Metropolis et al. 1953), and the goodness of fit measured by changes in twice the log-likelihood score that asymptotically follows an χ^2 distribution with degrees of freedom equal to the change in the value of model parameters (Edwards 1992).

Results

Original century parameterization (Orig)

Figure 4a shows the difference between the observed SOC (Fig. 3a) and the SOC prediction by the original Century formulation (Fig. 3b). The original Century parameters give rise to a latitudinal gradient in SOC qualitatively consistent with the observed global distribution of SOC, with large amounts of SOC in high latitudes and low amounts in tropical and temperate zones. However, the global latitudinal gradient is considerably stronger than observed, due to large over-estimation in many northern high latitude regions, including the Labrador Peninsula, the Pacific Northwest, Norway, Eastern coastal Siberia (Fig. 4a). Moreover, in boreal North America, the highest SOC density in the simulation occurs in the east and west of the continent, whereas the observations indicate that SOC values are highest in central boreal North America. At lower latitudes, under-estimation prevails: predictions for tropical areas such as Amazon, Central Africa, and South East Asia are generally lower than the observed values have less than 5 kg/m^2 SOC, compared to the more than 10 kg/m^2 in the observations. SOC in the Prairie grasslands of North America and Pampas of South America are also under-estimated.

Modified temperature dependency (Tdfit)

Optimization of the temperature dependency (Td) parameters (Eqs. 6–8) yields a significant improvement in the spatial distribution of SOC (Figs. 3c and 4b; Δl=9,900, P<0.001, Table 2). Compared to Orig, the standard error of the Tdfit model is 25.3% lower. In particular, the predictions for boreal and tundra regions are now closer to the observations, with the strong over-estimation of SOC in cold regions having reduced. However, this optimization still overestimates the SOC amount in the Labrador Peninsula and the Pacific Northwest of North America and eastern Siberia, and the under-estimation of tropical and temperate SOC accumulation are virtually unchanged from Orig.

Modified moisture dependency (Mdfit)

Modification of moisture dependency (Md) parameters (Eqs. 9 and 10) significantly improves the model's goodness of fit (Δl=2,050, P<0.001, Table 2). However, the resulting difference map (Figs. 3d and 4c) is similar to that obtained with Orig (Figs. 3b and 4a), and the standard error of the Mdfit model is only 0.04% lower, indicating that altering the moisture dependency parameters does not largely improve the model's predictive ability compared to Orig. High SOC densities are still predicted for higher latitudinal zones, and tropical and temperate SOC densities remain too low.

Modified temperature and moisture dependencies (TdMdfit)

Modifying both Md and Td yields a large improvement in the model's goodness of fit (Δl=22,000, P<0.001, Table 2), reducing the standard error of the TdMdfit model by 41.7% compared to Orig. Three factors contribute to the improved goodness-of fit (Figs. 3e and 4d). First, the over-estimation of SOC in the Labrador Peninsula, the northern Pacific coastal forests of North America, and the Tibetan Plateau is extensively reduced. Second, there is a significant increase in SOC in continental boreal regions, which is more consistent with the observations. Third, the under-estimation of SOC in lower latitudinal regions such as tropics (e.g., Amazon, Central Africa, and Southeastern Asia) and grasslands (e.g., Prairie and Pampas) is reduced. In addition, several localized patterns of SOC accumulation in temperate and tropical regions, such as those in southern Chile and Myanmar, are now reproduced.

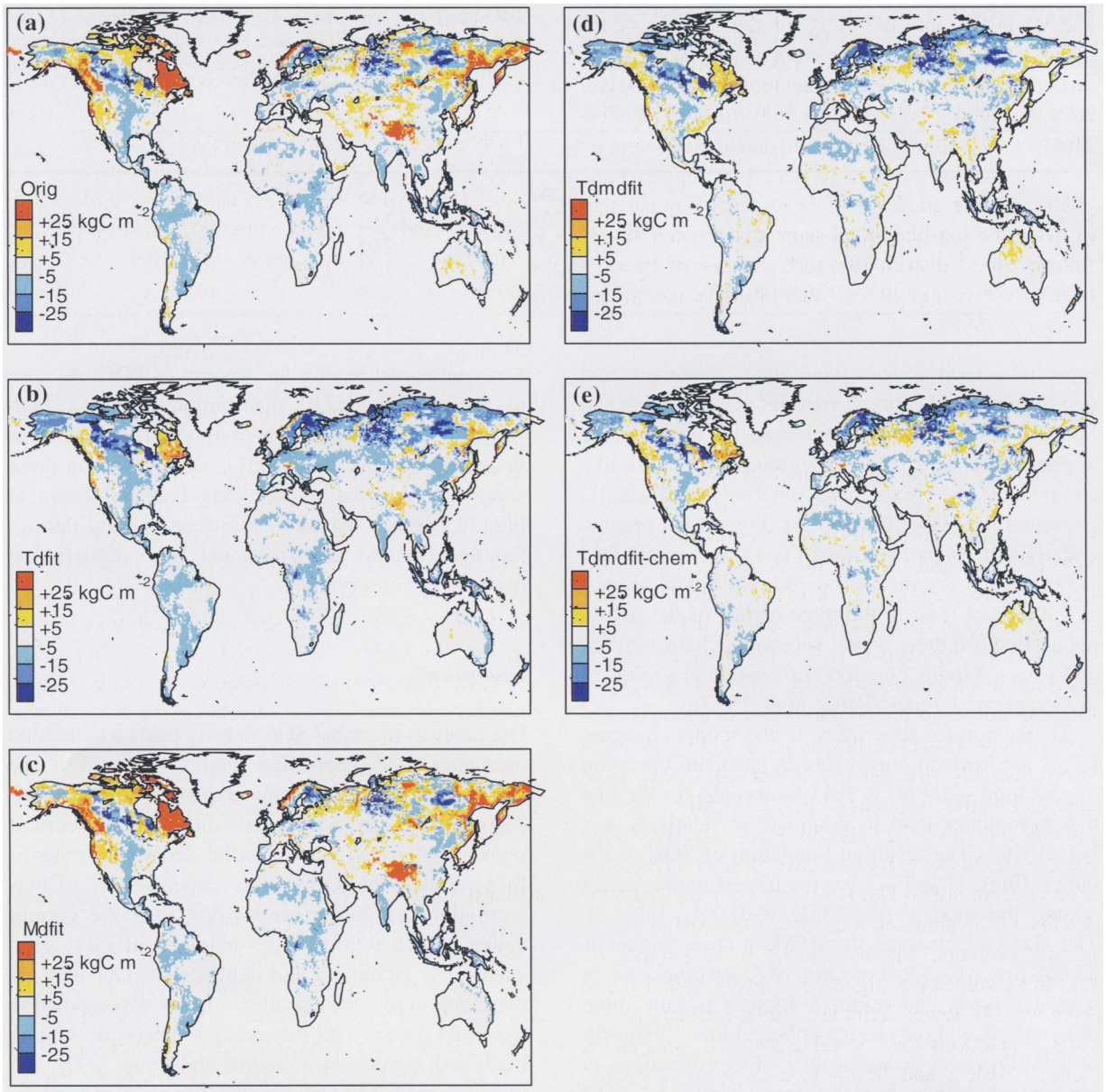

Fig. 4 Prediction difference [kgC m^{-2}] from observation (Global Soil Data Task 2000). Areas of over-estimation are presented in shades of red, and areas of under-estimation are in shades of blue. (**a**) Orig: Original Century parameters. (**b**) Tdfit: optimized temperature dependency. (**c**) Mdfit: optimized moisture dependency. (**d**) TdMdfit: optimized temperature and moisture dependencies. (**e**) TdMdfit-chem: optimized temperature and moisture dependencies with altered litter chemistry in lowland boreal region

Modified temperature and moisture dependencies with boreal litter chemistry (TdMdfit-chem)

While the amount of SOC in boreal regions predicted by the TdMdfit is closer to the observed values than either Orig, Tdfit, or Mdfit, the model still underestimates the amount of boreal SOC. For example, a band of high SOC accumulation in Canadian boreal region (Fig. 3a) is not fully reproduced by TdMdfit (Fig. 3e). A plausible explanation for this is the particular chemical characteristics of litter in boreal forests: boreal coniferous forests have a significantly different litter quality compared to temperate coniferous forests due to the understory dominance by

Table 2 Comparison of model trials. Orig: original Century parameters (without parameter fitting). Tdfit: with parameter fitting of temperature dependence (Td). Mdfit: with parameter fitting of moisture dependence (Md). TdMdfit: with parameter fitting of temperature and moisture dependence (Td and Md). TdMdfit-chem: with parameter fitting of temperature and moisture dependence (Td and Md) with alternative boreal C:N ratio and lignin fraction. Δl is the change in log likelihood from Orig, which has $l=-139{,}755$

Trials	Δl (P-value)	td_a	td_b	md_a	md_b
Orig	0 (–)	0.200	2.63	30.0	8.50
Tdfit	9,900 (<0.01)	0.302	1.93	30.0	8.50
Mdfit	2,050 (<0.01)	0.200	2.63	10.6	4.73
TdMdfit	22,000 (<0.01)	0.238	1.71	10.1	2.04
TdMdfit-chem	23,000 (<0.01)	0.101	2.34	10.2	1.97

bryophytes such as *Sphagnum* whose decomposition rate is only 1–10% that of vascular plants (Bonan and Shugart 1989). The primary reason for recalcitrance appears to be their high concentrations of lignin-like compounds. For example, Scheffer et al. (2001) estimated that the fraction of lignin-like organic materials in *Sphagnum* mosses is 43% of total SOC. However, the chemical properties for boreal biomes in the dataset used in the three earlier model fits do not account for these boreal vegetation characteristics and uses a Lignin Fraction (LF) identical to that of the temperate biomes (Potter et al. 1993).

To account for this, we re-fit the model changing LF of the lowland boreal forests (standard deviation of elevation <200 m) to 0.43 to account for the fact that bryophytes tend to dominate in relatively wet boreal sites. The resulting prediction of SOC distribution (Figs. 3f and 4e) has the largest improvement among the models (Δl=23,000, P<0.001, Table 2). The standard error of the TdMdfit-chem model is 42.6% lower than that of Orig. SOC accumulation in central Canada and northern Eurasia is now more pronounced, and the change in boreal litter chemistry in TdMdfit-chem does not alter SOC estimations in biomes other than boreal forests. Simulated SOC densities in tundra, temperate, and tropical regions are generally consistent with the observed data, similar to TdMdfit. Over-estimation of SOC in the Labrador Peninsula and in the northern Pacific coastal forests of North America is still apparent, however.

Overall, TdMdfit-chem yields reasonable predictions for the majority of global land surface. Based on the comparison plots (Fig. 5) the recalibrated model predicts SOC density well up to 20 kgC m^{-2} (Fig. 5c), which, as shown in Fig. 5b, covers 84% of the observations. However, above 20 kgC m^{-2}, the model continues to perform inadequately, consistently under-estimating the amount of SOC. As seen in the observed SOC distribution (Fig. 3a), high values of SOC are concentrated in boreal regions indicating that the model still underperforms in these areas. The residuals of the Orig that are shown in Fig. 5d indicate that the gamma probability density function captures the occasional large outliers that occur in the observations.

Discussion

Our analysis of global SOC density using a simplified mechanistic decomposition model implies that the global-scale environmental dependencies of SOC decomposition are significantly different from current representations within terrestrial ecosystem models. In particular, the temperature dependencies of heterotrophic respiration are weaker than the current values, which reflect values obtained in short-term, small-scale laboratory and field studies. Our findings therefore imply that acceleration in decomposition rates that occurs with increasing temperature will be likely less significant (Giardina and Ryan 2000) than previous predictions of terrestrial ecosystem models. The Td curves used in Orig (original Century parameters), TdMdfit, and TdMdfit-chem simulations are plotted in Fig. 6a. Q_{10} values of temperature sensitivity for the range of 0–30°C is 1.37 compared to 2.49 for Orig and 2.08 for Tdfit. The steep temperature dependency of the original Century parameters causes SOC over-estimation in tundra and other cold regions where soil temperatures remain low throughout the year, in spite of low NPP, implying that the predicted decomposition rates of the original Century formulation in cold regions are too slow.

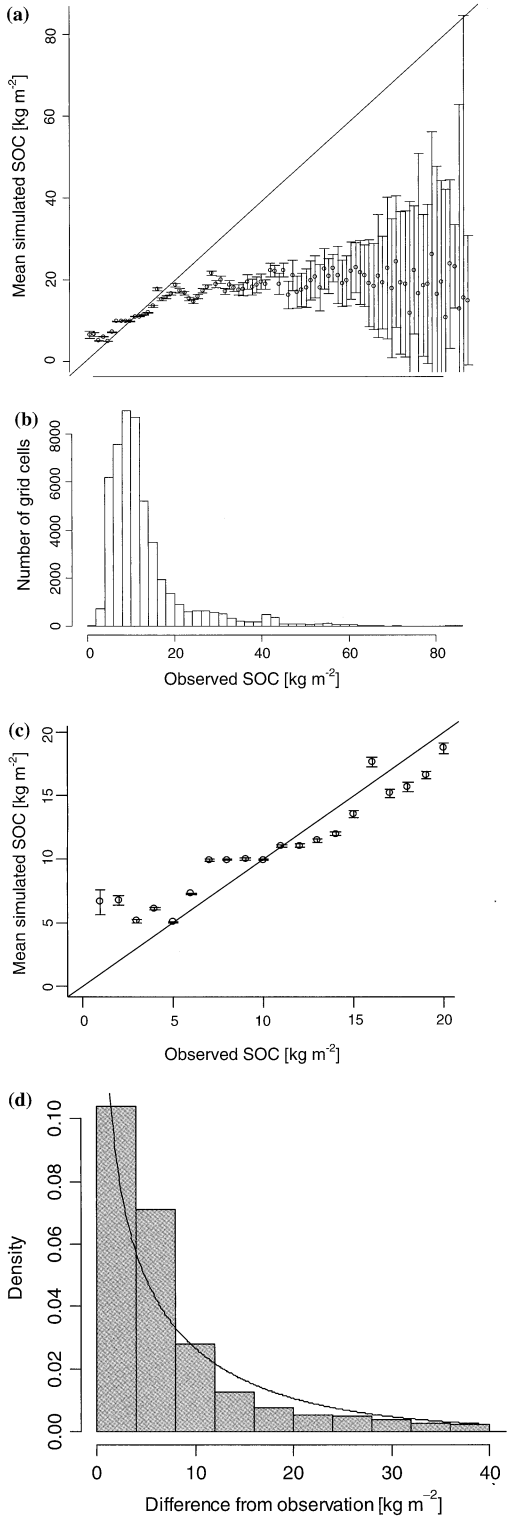

Fig. 5 Comparison between simulation (TdMdfit-chem) and observed data (Global Soil Data Task 2000). (**a**) Simulated values are binned and averaged for observational data with 1 kg m^{-2} interval. A 1:1 line is shown. (**b**) Distribution of grid cells. Eighty-four percent of grid cells have SOC of less than 20 kg m^{-2}. (**c**) A close-up of the figure to show the general agreement of simulated and observed values up to 20 kg m^{-2}. (**d**) Error distribution of Orig and a fitted gamma density distribution (estimated parameter: a=0.577 and b=15.9. Standard deviation=7.19)

This is perhaps not surprising since the original Century was developed for temperate climates (Parton et al. 1987), while tundra and other cold areas tend to fall at the lower end of the temperature dependency curve. In addition, the Q_{10} concept that underpins the original Century formulation assumes conditions of excess substrate and stable enzyme quantity and quality – conditions that are almost certainly not met when considering global-scale variation in decomposition rates. Both substrates and enzymes (microbes) are highly heterogeneous in terms of temporary and spatially, and decomposition rate may not respond to temperature as described by small-scale studies. In particular, recent studies suggest that acclimatory decreases in the temperature sensitivity of soil respiration occur (Luo et al. 2001; Melillo et al. 2002). In addition, changes in the microbial composition of decomposer community may reduce the latitudinal variability of SOC decomposition (Valentini et al. 2000).

The parameter fitting also indicates a different optimal moisture condition for SOC decomposition than the original Century parameterization (Parton et al. 1987, Fig. 6b). The optimal moisture condition in TdMdfit-chem occurs at PPT/PET=1.70, a substantially wetter condition than the original Century model in which decomposition is maximal when PPT/PET=1.0. To verify whether the optimum PPT/PET≠1.0 is significant, a TdMdfit-chem fit is performed with a prescribed optimum PPT/PET of 1.0. The change in log-likelihood for this simulation (Δl=8,960) is significantly smaller than that of a TdMdfit-chem simulation with a flexible optimum PPT/PET, and we can conclude that optimum moisture condition for SOC decomposition in this study is much higher than previously thought. One explanation for this may be the absence of an explicit consideration of runoff. A simple description of terrestrial water budget under equilibrium condition

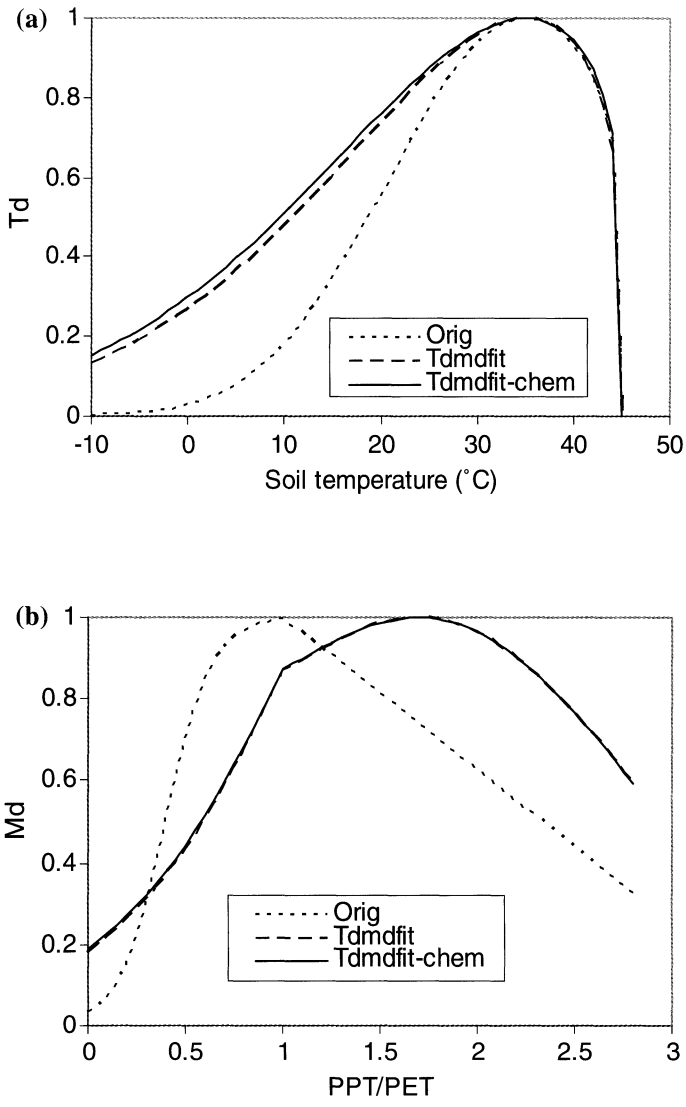

Fig. 6 Comparison of (**a**) temperature and (**b**) moisture dependence curves among Orig, TdMdfit, and TdMdfit-chem

is PPT=AET+*R* (Dingman 2002) where PPT is precipitation, AET is actual evapotranspiration, and *R* is runoff. Under high moisture conditions, $AET \approx PET$, and in the absence of runoff, PPT/PET>1 implies saturated soil conditions and thus low rates of decomposition. However, the occurrence of runoff will mean that in reality the onset of saturated conditions and the resulting slowing down of decomposition will only arise at PPT/PET ratios considerably higher than 1. Further exploration of this issue requires moving beyond the simple formulation analyzed here, to newer formulations such as the latest version of the Century model that explicitly incorporates the effects of runoff (Metherell et al. 1993).

To assess the implications of these altered temperature and moisture dependencies for atmospheric CO_2 concentrations, we simulated a uniform global climate warming of 1°C in the TdMdfit-chem model, and found that the temperature rise caused a loss of 2.8% of the global SOC. With a model with an equilibrium assumption, Potter and Klooster (1997) found that the uniform global warming of 1°C caused a loss of 5% of the global SOC. Our prediction of the enhancement of SOC loss due to the temperature rise is thus significantly smaller than that by Potter and Klooster (1997), reflecting the modified temperature dependency. Note that these are predictions for equilibrium soil conditions, which may take additional decades after changes in temperature. Under a tem-

perature rise of 2.6°C, the anticipated temperature rise in this century (IPCC 2001), TdMdfit-chem dependency parameters predicts 5.4% SOC loss. In a similar manner, changing the Q_{10} from 2.0 to 1.37 would lead to a significant reduction in the SOC feedbacks in the coupled model simulations of Cox et al. (2000).

The mean ages of decomposing CO_2 fluxes implied by the model fits compare reasonably with the observed values: the simulated mean ages of decomposing CO_2 fluxes from tropical, temperate, and boreal forests are 9.4, 17.6, and 43.9 years, respectively. While estimated ages of decomposing SOC by Trumbore (2000) are lower than our model predictions (3, 8, and 30 years for tropical, temperate, and boreal forests), this likely is due to the difference in the depth of SOC: Trumbore only considered SOC to a depth of 40 cm, here we model SOC to a depth of 100 cm. However, further validation with the global empirical model of soil respiration, including root respiration as well as heterotrophic respiration, such as Raich et al. (2002) would be beneficial.

An important assumption in this analysis is that the global environmental dependencies of decomposition estimated from spatial variations in temperature, moisture, and SOC are good predictors of temporal changes in decomposition expected from global climate change. The justification for this approach is the ubiquitous dispersal of microbial species in soil communities (Finlay 2002). Since the abundance of microbial species is not restricted by geographical barriers, appropriate soil microbial communities for decomposition will soon develop under the change in climate. This view also supports long-term acclimatization of soil decomposition (Luo et al. 2001; Melillo et al. 2002).

While the analysis performed here takes account for the effects of land-use on SOC, it does not account for transient changes in SOC that can occur as a result of land-use history. For example, a conversion from pristine ecosystem to agricultural field may cause gradual loss of SOC (Bellamy et al. 2005; Schulze and Freibauer 2005), and thus SOC under cultivation may not be in equilibrium. Large-scale land-use change has occurred in areas such as Prairie of North America, the black soil band of central Europe and Russia, and Pampas of South America. These areas that historically accumulated relatively large amounts of SOC are now gradually losing SOC due to land conversion (Gitz and Ciais 2004). Our model may under-estimate the amount of SOC in those areas because the model assumes an equilibrium SOC obtained under cultivation.

As in the original Century formulation, the model analyzed here assumes that the environmental dependencies of the decomposition rates of the metabolic, structural, and slow/passive SOC pools are identical, that SOC pools are not vertically stratified, and thus that above- and below-ground litter inputs are not distinguished. The shared environmental dependencies of the different SOC pools are supported by results of several studies that indicate that the different SOC pools have similar temperature sensitivities (Burke et al. 2003; Fang et al. 2005). However, results from other studies suggest that the temperature sensitivity of decomposition varies between different SOC pools (Bellamy et al. 2005; Fierer et al. 2005; Knorr et al. 2005; Leifeld and Fuhrer 2005), and that the vertical distribution of SOC can influence decomposition rates (Jobbagy and Jackson 2000). Also, similar to many global-scale models (e.g., Jones et al. 2005), the decomposition model formulation does not vary between terrestrial biomes or with soil type. In natural ecosystems, forest floor SOC and mineral soil SOC are affected by distinct groups of macrofauna, humification in organic soil is more pronounced than in mineral soil (Clymo 1984), and clay contents of mineral soil affect decomposition dynamics (Parton et al. 1987). An interesting topic for future analyses would be to compare the predictions of decomposition models that incorporate these different sources of heterogeneity in decomposition rates, including consideration of different environmental sensitivities for different SOC pools. Finally, the fit of the model TdMdfit-chem model would likely be further improved by utilizing more detailed land-cover datasets such as the LUCIA dataset (Kerr and Cihlar 2003) for the Canadian boreal region that classifies boreal coniferous forests into four categories.

Acknowledgements We appreciate the helpful comments from Professor Michael G. Ryan and Dr. Christian P. Giardina. The graduate study of Takeshi Ise is supported by the James Mills Peirce Fellowship provided by the Department of Organismic and Evolutionary Biology at Harvard University. Comments from anonymous reviewers have clarified the manuscript, and suggestions and discussions on the Q_{10} concept and other fundamental assumptions are extremely valuable.

References

Bachelet D, Lenihan JM, Daly C, Neilson RP, Ojima DS, Parton WJ (2001) MC1: A dynamic vegetation model for estimating the distribution of vegetation and associated ecosystem fluxes of carbon, nutrients and water. USDA Forest Service General Technical Report, PNW-GTR-508 1-95

Bellamy PH, Loveland PJ, Bradley RI, Lark RM, Kirk GJD (2005) Carbon losses from all soils across England and Wales 1978–2003. Nature 437:245–248

Bolker BM, Pacala SW, Parton WJ (1998) Linear analysis of soil decomposition: insights from the Century model. Ecol Appl 8:425–439

Bonan GB, Shugart HH (1989) Environmental-factors and ecological processes in boreal forests. Annu Rev Ecol Syst 20:1–28

Burke I, Kaye J, Bird S, Hall S, McCulley R, Sommerville G (2003) Evaluating and testing models of terrestrial biogeochemistry: the role of temperature in controlling decomposition. In: Canham C, Cole J, Lauenroth W (eds) Models in ecosystem science. Princeton Univ. Press, NJ, pp 225–253

Chimner RA, Welker JM (2005) Ecosystem respiration responses to experimental manipulations of winter and summer precipitation in a Mixedgrass Prairie, WY, USA. Biogeochemistry 73:257–270

Clymo RS (1984) The limits to peat bog growth. Philos Trans Royal Soc B 303:605–654

Cox P (2001) Description on the triffid dynamic global vegetation model. Technical Report 24. Hadley Centre Met Office, Devon UK

Cox PM, Betts RA, Jones CD, Spall SA, Totterdell IJ (2000) Acceleration of global warming due to carbon-cycle feedbacks in a coupled climate model. Nature 408: 184–187

Cramer W, Kicklighter DW, Bondeau A, Moore B, Churkina C, Nemry B, Ruimy A, Schloss AL (1999) Comparing global models of terrestrial net primary productivity (NPP): overview and key results. Global Change Biol 5(Suppl 1):1–15

Dai A, Fung IY (1993) Can climate variability contribute to the ''missing'' CO_2 sink?. Global Biogeochem Cy 7:599–609

Dingman SL (2002) Physical hydrology, 2nd edn. Prentice Hall, Upper Saddle River, NJ

Edwards AWF (1992) Likelihood. John Hopkins University Press, Baltimore

Environment Canada (1995) The state of Canada' s climate: monitoring change and variability. SOE Report No. 95-1 (p 52). Ottawa, Canada

Fang CM, Smith P, Moncrieff JB, Smith JU (2005) Similar response of labile and resistant soil organic matter pools to changes in temperature. Nature 433:57–59

Fierer N, Craine JM, McLauchlan K, Schimel JP (2005) Litter quality and the temperature sensitivity of decomposition. Ecology 86:320–326

Finlay BJ (2002) Global dispersal of free-living microbial eukaryote species. Science 296:1061–1063

Foley JA, Prentice IC, Ramankutty N, Levis S, Pollard D, Sitch S, Haxeltine A (1996) An integrated biosphere model of land surface processes, terrestrial carbon balance, and vegetation dynamics. Global Biogeochem Cy 10:603–628

Friedlingstein P, Delire C, Muller JF, Gerard JC (1992) The climate induced variation of the continental biosphere: a model simulation of the Last Glacial Maximum. Geophys Res Lett 19:897–900

Giardina CP, Ryan MG (2000) Evidence that decomposition rates of organic carbon in forest mineral soil do not vary with temperature. Nature 404:858–861

Gitz V, Ciais P (2004) Future expansion of agriculture and pasture acts to amplify atmospheric CO_2 levels in response to fossil-fuel and land-use change emissions. Clim Change 67:161–184

Global Soil Data Task (2000) Global soil data products CD-ROM (IGBP-DIS). International Geosphere-Biosphere Programme – data and information services. Available online at [http://www.daac.ornl.gov/] from the ORNL Distributed Active Archive Center, Oak Ridge National Laboratory, Oak Ridge, TN

Gorham E (1991) Northern peatlands – role in the carbon-cycle and probable responses to climatic warming. Ecol Appl 1:182–195

Hansen J, Fung I, Lacis A, Lebedef S, Rind D, Ruedy R, Russel G, Stone P (1988) Global climate changes as forecast by the Goddard Institute for Space Studies three dimensional model. J Geophys Res 93:9341–9364

Holland EA, Neff JC, Townsend AR, McKeown B (2000) Uncertainties in the temperature sensitivity of decomposition in tropical and subtropical ecosystems: implications for models. Global Biogeochem Cy 14:1137–1151

Intergovernmental Panel on Climate Change (2001) Climate change 2001: the scientific basis. Available online at [http://www.grida.no/climate/ipcc_tar/]

Jobbagy EG, Jackson RB (2000) The vertical distribution of soil organic carbon and its relation to climate and vegetation. Ecol Appl 10:423–436

Jones CD, Cox PM, Essery RLH, Roberts DL, Woodage MJ (2003) Strong carbon cycle feedbacks in a climate model with interactive CO_2 and sulphate aerosols. Geophys Res Lett 30:1479, doi:10.1029/2003GL016867

Jones C, McConnell C, Coleman K, Cox P, Falloon P, Jenkinson D, Powlson D (2005) Global climate change and soil carbon stocks; predictions from two contrasting models for the turnover of organic carbon in soil. Glob Change Biol 11:154–166

Kirschbaum MUF (1995) The temperature dependence of soil organic matter decomposition, and the effect of global warming on soil organic C storage. Soil Biol Biochem 27:753–760

Kerr JT, Cihlar J (2003) Land use and cover with intensity of agriculture for Canada from satellite and census data. Global Ecol Biogeog 12:161–172

Knorr W, Prentice IC, House JI, Holland EA (2005) Long-term sensitivity of soil carbon turnover to warming. Nature 433:298–301

Leifeld J, Fuhrer J (2005) The temperature response of CO_2 production from bulk soils and soil fractions is related to soil organic matter quality. Biogeochemistry 75:433–453

Lieth H (1975) Modeling the primary productivity of the world. In: Lieth H, Whittaker RH (eds) Primary Productivity of the biosphere. Springer-Verlag, New York, pp 237–263

Luo Y, Shiqiang W, Dafeng H, Wallace LL (2001) Acclimatization of soil respiration to warming in a tall grass prairie. Nature 413:622–625

Malmstrom VH (1969) A new approach to the classification of climate. J Geog 68:351–357

Manabe S, Wetherald RT (1987) Large scale changes in soil wetness induced by an increase in carbondioxide. J Atmos Sci 44:1211–1235

Melillo JM, Steudler PA, Aber JD, Newkirk K, Lux H, Bowles FP, Catricala C, Magill A, Ahrens T, Morrisseau S (2002) Soil warming and carbon-cycle feedbacks to the climate system. Science 298:2173–2176

Metherell AK, Harding LA, Cole CV, Parton WJ (1993) CENTURY soil organic matter model environment: technical documentation. Agroecosystem version 4.0. Great Plains System Res Unit Tech Report 4. USDA-ARS, Fort Collins, CO, USA

Metropolis N, Rosenbluth AW, Rosenbluth MN, Teller AH, Teller E (1953) Equations of state calculations by fast computing machines. J Chem Phys 21:1087–1091

Moorcroft PR, Hurtt GC, Pacala SW (2001) A method for scaling vegetation dynamics: the ecosystem demography model (ED). Ecol Monogr 71:557–585

New M, Hulme M, Jones PD (2000) Global 30-year mean monthly climatology, 1961–1990 data set. Available online [http://www.daac.ornl.gov] from Oak Ridge National Laboratory Distributed Active Archive Center, Oak Ridge, TN

Niklinska M, Maryanski M, Laskowski R (1999) Effect of temperature on humus respiration rate and nitrogen mineralization: implications for global climate change. Biogeochemistry 44:239–257

Parton WJ, Schimel DS, Cole CV, Ojima DS (1987) Analysis of factors controlling soil organic matter levels in Great Plains grasslands. Soil Sci Soc Am J 51:1173–1179

Parton WJ, Scurlock JMO, Ojima DS, Gilmanov TG, Scholes RJ, Schimel DS, Kirchner T, Menaut JC, Seastedt T, Moya EG, Kamnalrut A, Kinyamario JI (1993) Observations and modeling of biomass and soil organic-matter dynamics for the grassland biome worldwide. Global Biogeochem Cy 7:785–809

Parton W, Stewart J, Cole C (1988) Dynamics of C, N, P and S in grassland soils – a model. Biogeochemistry 5:109–131

Potter CS, Klooster SA (1997) Global model estimates of carbon and nitrogen storage in litter and soil pools: response to changes in vegetation quality and biomass allocation. Tellus B 49:1–17

Potter CS, Randerson JT, Field CB, Matson PA, Vitousek PM, Mooney HA, Klooster SA (1993) Terrestrial ecosystem production: a process model based on global satellite and surface data. Global Biogeochem Cy 7:811–841

Raich JW, Potter CS, Bhagawati D (2002) Interannual variability in global soil respiration, 1980–94. Glob Change Biol 8:800–812

Ramankutty N, Foley JA (1998) Characterizing patterns of global land use: an analysis of global croplands data. Global Biogeochem Cy 12:667–685

Scheffer RA, van Logtestijn RSP, Verhoeven JTA (2001) Decomposition of *Carex* and *Sphagnum* litter in two mesotrophic fens differing in dominant plant species. Oikos 92:44–54

Schimel DS, Braswell BH, Holland EA, McKeown R, Ojima DS, Painter TH, Parton WJ, Townsend AR (1994) Climatic, edaphic, and biotic controls over storage and turnover of carbon in soils. Global Biogeochem Cy 8:279–293

Schimel DS, Braswell BH, McKeown R, Ojima DS, Parton WJ, Pulliam W (1996) Climate and nitrogen controls on the geography and timescales of terrestrial biogeochemical cycling. Global Biogeochem Cy 10:677–692

Schlesinger WH (1997) Biogeochemistry, an analysis of global change. Academic Press, San Diego, CA

Schlesinger ME, Zhao ZC (1988) Seasonal climatic changes induced by doubled CO_2 as simulated by the OSU atmospheric GCM/mixed layer ocean model. Climate Research Institute, Oregon State University, Corvallis, OR

Schulze ED, Freibauer A (2005) Carbon unlocked from soils. Nature 437:205–206

Stocks BJ, Fosberg MA, Lynham TJ, Mearns L, Wotton BM, Yang Q, Jin JZ, Lawrence K, Hartley GR, Mason JA, McKenney DW (1998) Climate change and forest fire potential in russian and canadian boreal forests. Clim Change 38:1–13

Trumbore S (2000) Age of soil organic matter and soil respiration: radiocarbon constraints on belowground C dynamics. Ecol Appl 10:399–411

Valentini R, Matteucci G, Dolman AJ, Schulze ED, Rebmann C, Moors EJ, Granier A, Gross P, Jensen NO, Pilegaard K, Lindroth A, Grelle A, Bernhofer C, Grunwald T, Aubinet M, Ceulemans R, Kowalski AS, Vesala T, Rannik U, Berbigier P, Loustau D, Guomundsson J, Thorgeirsson H, Ibrom A, Morgenstern K, Clement R, Moncrieff J, Montagnani L, Minerbi S, Jarvis PG (2000) Respiration as the main determinant of carbon balance in european forests. Nature 404:861–865

Yang X, Wang M, Huang Y, Wang Y (2002) A one-compartment model to study soil carbon decomposition rate at equilibrium situation. Ecol Model 151:63–73

Winkler JP, Cherry RS, Schlesinger WH (1996) The Q_{10} relationship of microbial respiration in a temperate forest soil. Soil Biol Biochem 28:1067–1072